ELSEVIER

Journal of Nuclear Materials 307–311 (2002) 236–239

journal of nuclear materials

www.elsevier.com/locate/jnucmat

Assessment of mechanical properties of the martensitic steel EUROFER97 by means of punch tests

Y. Ruan, P. Spätig *, M. Victoria

Fusion Technology – Centre de Recherches en Physique des Plasmas, Ecole Polytechnique Fédérale de Lausanne, CH-5232 Villigen PSI, Switzerland

Abstract

The ball punch test technique was used to evaluate the conventional tensile and impact properties of the tempered martensitic steel EUROFER97 from room temperature down to liquid nitrogen temperature. The testing was carried out on unirradiated material only with small disks, 3 mm in diameter and 0.25 mm in thickness. For comparison, tensile tests were also performed over the same temperature range. Correlations between the load at the plastic bending initiation and the maximum load of the punch tests with the yield stress and the ultimate tensile stress of the tension tests could be established. The temperature dependence of the specific fracture energy of the punch test was used to define a ductile–brittle transition temperature (DBTT) and to correlate this with the DBTT measured from impact Charpy on KLST specimens. The results are compared with other available correlations done in the past on other ferritic steels.

1. Introduction

The ball and shear punch test techniques have been developed to extract the tensile properties [1], the so-called ductile–brittle transition temperature (DBTT) as measured by Charpy impact [2] and the fracture properties [3,4]. While the reasons to develop such small specimen techniques are many, the development of such techniques has been mainly driven by the need to minimize the specimen size due to the space limitation of the current irradiation facilities but also by the relatively limited irradiation volume of the anticipated high energy neutron source for fusion materials. Among the material candidates for the fusion reactor structures, the tempered martensitic steels are the most advanced materials [5]. It was already shown that those steels remain stable under irradiation up to very high doses (200 dpa) [6] but the effect of the large quantity of gas (H, He) produced by transmutation on the fracture properties are still open issues. In conjunction with other small specimen techniques, it is planned to use the ball punch test technique to assess the He effect on fracture by testing irradiated material containing different He contents but with the same damage level. One way to achieve that goal is to perform neutron irradiations in reactor in parallel to high energy proton (590 MeV) irradiation with PIREX facility at PSI [7]. Indeed, when irradiated with 590 MeV protons, the He generation rate in the tempered martensitic steels is very high, of the order of 100 appm He/dpa, that is about one order of magnitude more than what will be produced by 14 MeV neutrons.

The work presented in this communication was done on the reduced activation tempered martensitic steel EUROFER97, which belongs to the 7–9Cr class of steel. The results reported were obtained in the unirradiated material at low temperature. The objective was to establish the correlations between, on the one hand, the tensile data (yield stress, ultimate tensile strength) with the punch test results and, on the other hand, between the DBTT obtained from the Charpy tests with the specific energy of the punch deformation curve. This preliminary analysis has to be considered as a first step in the development of a more sophisticated analysis method making use of finite element calculations to model the plastic flow and fracture toughness under

* Corresponding author. Tel.: +41-56 310 2934; fax: +41-56 310 4529.

E-mail address: philippe.spatig@psi.ch (P. Spätig).

0022-3115/02/$ - see front matter
PII: S0022-3115(02)01194-7

complex multi-axial stress state. The punch test results reported here represent the general trend for the EUROFER97 but this data base need to be extended in the future to draw more quantitative conclusions on the mechanical properties.

2. Experimental

The alloy in this study is the reduced activation EUROFER97 steel, heat E83697, produced by Böhler AG. This steel contains 8.90 wt% Cr, 0.12 wt% C, 0.46 wt% Mn, 1.07 wt% W, 0.2 wt% V, 0.15 wt% Ta and Fe for the balance. The steel was heat-treated by normalizing at 1253 K for 0.5 h and tempering at 1033 K for 1.5 h. The steel was fully martensitic after quenching. The prior austenite grain size was about 10 (ASTM) [8].

Tensile tests were performed on round specimens 3 mm in diameter and 18 mm in gauge length. The tests were carried out on a MTS servo-hydraulic machine at constant nominal strain rates of 5×10^{-4} s^{-1} in the temperatures range from 80 to 293 K. Temperature control was provided by either a liquid-nitrogen-cooled alcohol bath or a regulated N_2 gas environment. Small punch tests were performed on an electro-mechanical Schenck RMC100 machine. The load was applied to a 3 mm diameter, 0.25 mm thick disk specimen with a steel ball of 1 mm diameter. In order to control the temperature below room temperature, a bath of ethanol or methyl butane was used in which the punch die was immerged. A good temperature stability was achieved over the temperature range 133–293 K and at 80 K. However, it was not sufficient from 80K up to 133 K; as a consequence, no data point are reported here between these two last temperatures.

3. Results and discussion

A typical load-deflection curve at room temperature obtained at room temperature is presented in Fig. 1. As observed previously on other type of steels [9,10], the curves can be divided in four stages, namely: I elastic bending, II plastic bending, III, plastic membrane stretching and IV plastic instability. The nature of the deformation mechanisms associated to the different regimes was presented in details by Manahan et al. [11]. These four deformation regimes are indicated in Fig. 1 along with the load associated to the initialization of the plastic straining, P_y and the maximum load, P_{max}. In order to establish a mathematical relationship between, on the one hand, P_y and the yield stress $\sigma_{0.2}$, and, on the other hand, P_{max} and the ultimate tensile strength (UTS), P_y, and P_{max} were systematically divided by t_o^2, where t_o is the thickness of the specimen. The temperature dependence of the normalized yield load, P_y/t_o^2, and the normalized maximum load, P_{max}/t_o^2 is presented in Figs. 2 and 3 respectively. For direct comparison, $\sigma_{0.2}$ is indicated in Fig. 2 while UTS is shown in Fig. 3. When more than one data point was obtained at a given temperature, namely 80, 133, 173 and 293 K, the mean value is reported in the Figs. 2 and 3 with the associated error bar. It is emphasized that the reported values at 80 K is the average of three measurements so that the low P_{max}/t_o^2 value is well established. P_y/t_o^2 appears to be strongly temperature dependent below 200 K while remaining almost constant above 200 K. This behavior is consistent with the thermally activated nature of the yield strength of this class of tempered martensitic steels, which also exhibits a strong and monotonous increase of the yield stress below a nominal temperature of about 200 K [12]. It is worth noting that the ratio between the yield stresses at 200 and 80 K is similar to that of P_y/t_o^2 between the same temperatures: $\sigma_{0.2}(80\ K)/\sigma_{0.2}(200\ K) = 1.75$ while $P_y t_o^{-2}(80\ K)/P_y t_o^{-2}(200\ K) = 1.9$. The temperature dependence of P_{max}/t_o^2 presented in

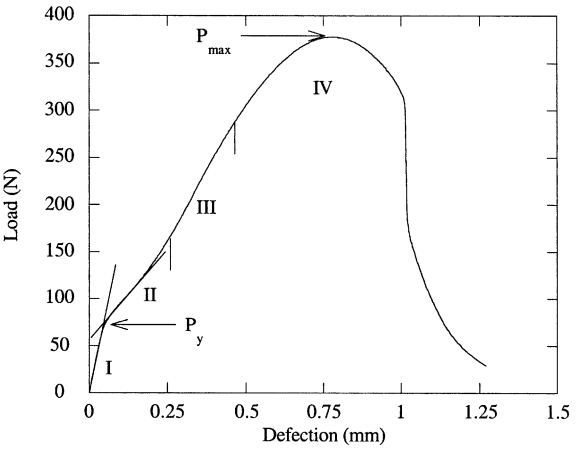

Fig. 1. Load–deflection curve at room temperature.

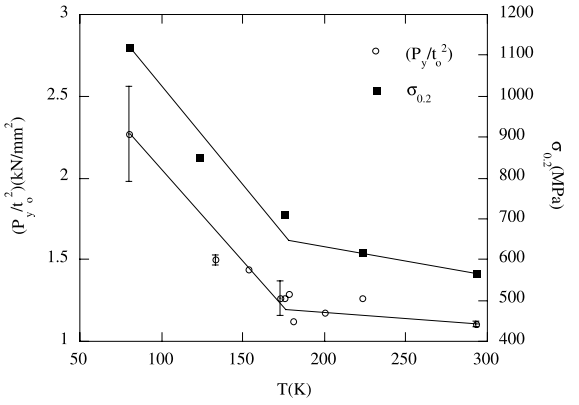

Fig. 2. Temperature dependence of P_y/t_o^2 and of $\sigma_{0.2}$.

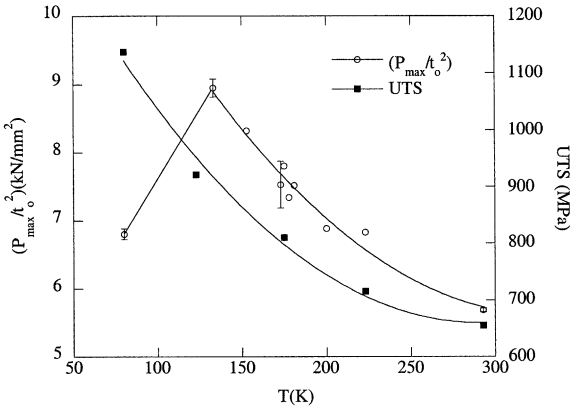

Fig. 3. Temperature dependence of P_{max}/t_o^2 and of UTS.

Fig. 3 differs significantly from that of P_y/t_o^2 in two ways. First, P_{max}/t_o^2 increases strongly from room temperature down to 133 K and second, below that last temperature it drops to reach a much lower value at 80 K. The temperature at which the maximum value of is attained is not yet precisely determined but it can be estimated to be 105 ± 25 K. Another relevant quantity can be deduced from the load–deflection curve, which is the specific fracture energy per unit specimen thickness (SFE), in mJ mm^{-1}. The SFE is shown in Fig. 4 as a function of temperature. The SFE gradually increases by decreasing temperature down to 133 K and suddenly drops at 80 K, similarly to P_{max}/t_o^2. Here again the temperature of the maximum for SFE is not precisely determined from the currently available data but it is also estimated to be 105 ± 25 K.

Based on the temperature dependence of the parameters presented in Figs. 2–4, empirical relationships can be established to extract the yield stress, the ultimate tensile stress and the DBTT as obtained from Charpy impact tests. Following the same methodology as Mao and Takahashi [10] to evaluate $\sigma_{0.2}$ and the UTS of a material by means of ball punch tests, the normalized yield load P_y/t_o^2 load and normalized maximum load P_{max}/t_o^2, are plotted in Fig. 5 as a function of $\sigma_{0.2}$ and UTS respectively obtained from plain tensile tests. Since it was observed that the temperature dependence of P_{max}/t_o^2 is not monotonous over the whole investigated temperature range like the UTS, we report in Fig. 5 only the data in the range (133–293 K) where both P_{max}/t_o^2 and the UTS vary similarly. However, as far as P_y/t_o^2 and $\sigma_{0.2}$ are concerned, it makes sense to plot one value against the other over the whole temperature range in the search of a simple relationship between them since both parameters vary in a similar manner. As can be seen in Fig. 5, linear relations can be used to predict the yield stress and the UTS from the ball punch parameters. These linear relationships read:

$$\sigma_{0.2}\ (\mathrm{MPa}) = (149 \pm 108) + (413 \pm 68)\frac{P_y}{t_o^2}\ (\mathrm{kN/mm^2}),$$
$$80 \leqslant T \leqslant 293\ \mathrm{K},$$

$$\mathrm{UTS}\ (\mathrm{MPa}) = (218 \pm 101) + (77 \pm 15)\frac{P_{max}}{t_o^2}\ (\mathrm{kN/mm^2}),$$
$$133 \leqslant T \leqslant 293\ \mathrm{K}.$$

In the above equations, the $\pm$ values represent the standard error values of the parameters.

The correlation between the DBTT and the punch test data was done by using the SFE values shown in Fig. 4. The plot of the SFE against temperature qualitatively exhibits some similar characteristics of the absorbed energy–temperature curve of a Charpy curve, even though the SFE decreases in the ductile domain. Due to the limitations in the cooling capability of the

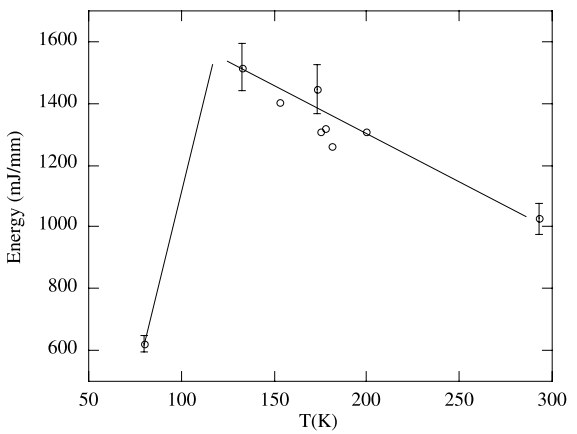

Fig. 4. Temperature dependence of the specific fracture energy.

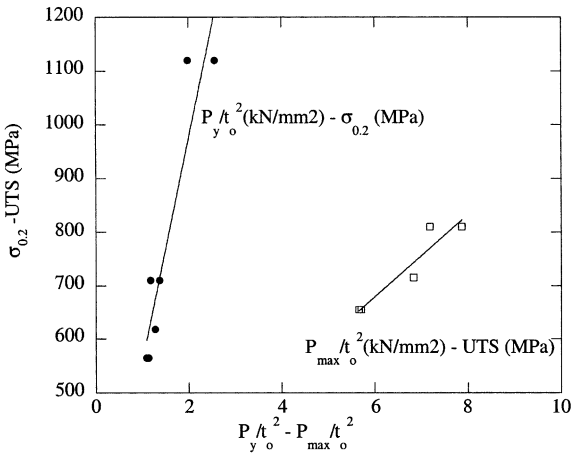

Fig. 5. Calibration between P_y/t_o^2–$\sigma_{0.2}$ and P_{max}/t_o^2–UTS.

testing device, it was not possible to perform tests below 80 K and the value of the lower shelf energy could not be attained. Therefore, if the DBTT of the ball punch tests $(DBTT)_{PT}$ is defined as the mean value of the lowest and highest fracture energies, the $(DBTT)_{PT}$ is estimated around 100 K or even lower. However, in the following, we used the same procedure as Moon et al. [13] and we define the $(DBTT)_{PT}$ at which the SFE is half the maximum value. In our case, this corresponds to 105 ± 25 K as discussed above. The DBTT measured by impact testing on KLST specimens was found equal to 198 K by Rensmann et al. [14]. For a series of ferritic steels, Kameda and Mao [15] found an empirical relationship between the DBTTs determined by small punch test and standard Charpy tests (STC); this relationship is $(DBTT)_{PT} = \alpha(DBTT)_{SCT}$, where $\alpha = 0.4$. While we dealt with KLST specimens in this study, we used the same type of calibration and we evaluated the parameter α by considering the above-mentioned values of $(DBTT)_{PT}$ and $(DBTT)_{KLST}$. In our case, we can write:

$$(DBTT)_{PT} = (0.52 \pm 0.12)(DBTT)_{KLST}.$$

The value of α is somewhat higher than that found by Kameda and Mao but the reason is probably due to the fact that the DBTT measured with KLST specimens is lower than that of standard specimens. Indeed, if we take $\alpha = 0.4$, the $(DBTT)_{SCT}$ is about 260 K, or in other words 62 K higher than $(DBTT)_{KLST}$. It is worth mentioning here that a shift of 50 K in the DBTT was observed between KLST and standard specimens in the tempered martensitic steel MANET II [16].

4. Summary

In this study, an attempt to assess the tensile and impact properties of the tempered martensitic steel EUROFER97 in the unirradiated condition by means of ball punch tests was done. The punch specimens were TEM disks, 3 mm in diameter and 0.25 mm in thickness. The punch testing was carried out from room temperature down to liquid nitrogen temperature with a machine piston velocity of 1 mm/min. The tensile testing used to compare the punch results to the usual tensile data were done over the same temperature domain and at a nominal strain rate of 5×10^{-4} s^{-1}. The characteristic loads associated to the initiation of the plastic bending domain, P_y, and the maximum load, P_{max}, were reported as a function of temperature and then compared to the temperature dependence of the yield stress, $\sigma_{0.2}$ and to the UTS obtained from plain tensile test. Linear relationships were established between, P_y/t_o^2 and $\sigma_{0.2}$ as well as P_{max}/t_o^2 and UTS. The specific fracture energy of the punch tests was also determined and reported as a function of temperature. It was observed to increase by decreasing temperature until a sharp decrease happens below 133 K. The DBTT obtained from the punch tests and defined as the temperature at which the energy is half the maximum value was compared to the DBTT determined form impact Charpy on KLST specimens. A fair agreement with previously reported data on other ferritic steels was found.

Acknowledgements

The financial support of EURATOM is gratefully acknowledged. The Paul Scherrer Institute is acknowledged for the overall use of facilities. The technical help of D. Gragg for the low temperature tensile testing, which was performed at the University California Santa Barbara in the group of Professor G.R. Odette, was greatly appreciated.

References

[1] G.E. Lucas, J.W. Sheckherd, G.R. Odette, S. Panchanadeeswaran, J. Nucl. Mater. 122&123 (1984) 429.
[2] S.H. Song, R.G. Faulkner, P.E.J. Flewitt, R.F. Smith, P. Marmy, Mater. Sci. Eng. A 281 (2000) 75.
[3] J.R. Foulds, P.J. Woytowitz, T.K. Parnell, C.W. Jewett, J. Testing Eval. 23 (1) (1995) 3.
[4] X. Mao, M. Saito, H. Takahashi, Scr. Metall. 25 (1991) 2481.
[5] M. Victoria, N. Baluc, P. Spätig, Nucl. Fusion 41 (8) (2001) 1047.
[6] D.S. Gelles, J. Nucl. Mater. 212–215 (1994) 714.
[7] P. Marmy, M. Daum, D. Gavillet, S. Green, W.V. Green, F. Hegedüs, S. Proennecke, U. Rohrer, U. Stiefel, M. Victoria, Nucl. Instrum. and Meth. B 47 (1990) 37.
[8] H.E. Hofmans, NRG Reports 20023/00.38153/P (2000).
[9] J.-M. Baik, J. Kamela, O. Buck, in: W.R. Corwin, G.E. Lucas (Eds.), The use of small-scale specimens for testing irradiated material, ASTM-STP 888, American Society for Testing and Materials, Philadelphia, PA, 1986, p. 92.
[10] X. Mao, H. Takahashi, J. Nucl. Mater. 150 (1987) 42.
[11] M.P. Manahan, A.E. Browning, A.S. Argon, O.K. Harling, in: W.R. Corwin, G.E. Lucas (Eds.), The use of small-scale specimens for testing irradiated material, ASTM-STP 888, American Society for Testing and Materials, Philadelphia, PA, 1986, p. 17.
[12] P. Spätig, G.R. Odette, G.E. Lucas, J. Nucl. Mater. 275 (1999) 324.
[13] J.C. Moon, K. Fukaya, Y. Nishiyama, M. Suzuki, M. Eto, JAERI-memo 04-230 (1992).
[14] J. Rensman, H.E. Hofmans, E.W. Schuring, J. van Hoepen, J.B.M. Bakker, R. den Boef, F.P. van den Broek, E.D.L. van Essen, these Proceedings.
[15] J. Kameda, X. Mao, J. Mater. Sci. 27 (1992) 983.
[16] P. Marmy, unpublished work.